Effective-action approach to a trapped Bose gas

Emil Lundh* and Jørgen Rammer
Department of Theoretical Physics, Umeå University, SE-901 87 Umeå
(Received 28 November 2001; revised manuscript received 22 May 2002; published 17 September 2002)

The effective-action formalism is applied to a gas of bosons. The equations describing the condensate and the excitations are obtained using the loop expansion for the effective action. For a homogeneous gas, the expansion in terms of the diluteness parameter is identified in terms of the loop expansion. The loop expansion and the limits of validity of the well-known Bogoliubov [J. Phys. (Moscow) **11**, 23 (1947)] and Popov, (Zh. Éksp. Teor. Fiz. **47**, 1759 (1964) [Sov. Phys. JETP **20**, 1185 (1965)]) equations are examined analytically for a homogeneous dilute Bose gas and numerically for a gas trapped in a harmonic-oscillator potential. The expansion to one-loop order, and hence the Bogoliubov equation, is shown to be valid for the zero-temperature trapped gas as long as the characteristic length of the trapping potential exceeds the *s*-wave scattering length.

DOI: 10.1103/PhysRevA.66.033607 PACS number(s): 03.75.Fi, 05.30.Jp

I. INTRODUCTION

The dilute Bose gas has been subject to extensive study for more than half a century, originally in an attempt to understand liquid He II, but also as an interesting many-body system in its own right. In 1947, Bogoliubov showed how to describe Bose-Einstein condensation as a state of broken symmetry, in which the expectation values of the field operators are nonvanishing due to the single-particle state of lowest energy being macroscopically occupied, i.e., the annihilation and creation operators for the lowest-energy mode can be treated as *c* numbers [1]. In modern terminology, the expectation value of the field operator is the order parameter and describes the density of the condensed bosons. In Bogoliubov's treatment, the physical quantities were expanded in the diluteness parameter $\sqrt{n_0 a^3}$, where n_0 denotes the density of bosons occupying the lowest single-particle energy state, and a is the *s*-wave scattering length, and Bogoliubov's theory is therefore only valid for homogeneous dilute Bose gases. The inhomogeneous Bose gas was studied by Gross [2] and Pitaevskii [3], who independently derived a nonlinear equation determining the condensate density. A field-theoretic diagrammatic treatment was applied by Beliaev to the zero-temperature homogeneous dilute Bose gas, showing how to go beyond Bogoliubov's approximation in a systematic expansion in the diluteness parameter $\sqrt{n_0 a^3}$ [4,5]; and also showing how repeated scattering leads to a renormalization of the interaction between the bosons. This renormalization was in Beliaev's treatment a cumbersome issue, where diagrams expressed in terms of the propagator for the noninteracting particles are intermixed with diagrams where the propagator contains the interaction potential. Beliaev's diagrammatic scheme was extended to finite temperatures by Popov and Faddeev [6], and was subsequently employed to extend the Bogoliubov theory to finite temperatures by incorporating terms containing the excited-state operators to lowest order in the interaction potential [7,8].

A surge of interest in the dilute Bose gas due to the experimental creation of gaseous Bose-Einstein condensates occurred in the mid-1990s [9]. The atomic condensates in the experiments are confined in external potentials, which poses new theoretical challenges; especially, the Beliaev expansion in the diluteness parameter $\sqrt{n_0 a^3}$ is untenable when the density is inhomogeneous. The renormalization of the potential was generalized to a trapped system by Proukakis *et al.* [10,11]. Leading-order corrections to the Gross-Pitaevskii equation for a trapped Bose gas were studied by Stenholm [12]. The finite temperature Beliaev-Popov theory was applied to a trapped gas by Fedichev and Shlyapnikov [13].

Recent experiments on trapped Bose gases have employed Feshbach resonances to probe the regime of large scattering length, and hence large values of the diluteness parameter [14,15]. It is therefore of importance to understand the low-density approximations to the exact equations of motion and the corrections thereto. In this paper, we shall employ the two-particle irreducible effective-action approach, and show that it provides an efficient systematic scheme for dealing with both homogeneous Bose gases and trapped Bose gases. We show how the effective-action formalism can be used to derive the equations of motion for the dilute Bose gas, and more important, that the loop expansion can be used to determine the limits of validity of approximations to the exact equations of motion in the trapped case.

The paper is organized as follows. The model and the two-particle irreducible effective-action approach are introduced in Sec. II. The homogeneous dilute Bose gas is considered in Sec. III, and it is shown that the effective-action approach proves efficient for deriving the familiar equations of motion. In Sec. IV, we demonstrate how the renormalization of the interaction potential due to repeated scattering is conveniently carried out in the effective-action formalism. In Sec. V, the effective-action approach is applied to the trapped Bose gas. The main results of the paper are presented in Sec. VI, where the equations of motion are solved numerically in order to assess the limits of validity of approximations to the

*Present address: Helsinki Institute of Physics, P. O. Box 64, FIN-00014 University of Helsinki, Finland.

exact equations of motion. Finally, in Sec. VII, we summarize and conclude.

II. EFFECTIVE ACTION FORMALISM FOR BOSONS

We consider a system of spinless bosons described by the action

$$S[\psi,\psi^\dagger]=\int d\mathbf{r}dt\,\psi^\dagger(\mathbf{r},t)[i\partial_t-H_0(\mathbf{r})+\mu]\psi(\mathbf{r},t) -\frac{1}{2}\int d\mathbf{r}d\mathbf{r}'dt\,\psi^\dagger(\mathbf{r},t)\psi^\dagger(\mathbf{r}',t)U(\mathbf{r}-\mathbf{r}') \times\psi(\mathbf{r}',t)\psi(\mathbf{r},t), \quad (1)$$

where ψ is the scalar field describing the bosons. Here, μ denotes the chemical potential, $H_0=\mathbf{p}^2/2m+V(\mathbf{r})$ is the one-particle Hamiltonian consisting of the kinetic term and an external potential, and $U(\mathbf{r})$ is the potential describing the interaction between the bosons. We have chosen units so that $\hbar=1$, but will restore $\hbar$ in final results. It will prove convenient to introduce a matrix notation whereby the field and its complex conjugate are combined into a two-component field $\phi=(\psi,\psi^\dagger)=(\phi_1,\phi_2)$.

The correlation functions of the Bose field are obtained from the generating functional

$$Z[\eta,K]=\int\mathcal{D}\phi\exp\left(iS[\phi]+i\eta^\dagger\phi+\frac{i}{2}\phi^\dagger K\phi\right), \quad (2)$$

by differentiating with respect to the source $\eta^\dagger=(\eta,\eta^*)=(\eta_1,\eta_2)$. In Eq. (2), matrix notation is implied in order to suppress the integrations over space and time variables. A two-particle source term K has been added to the action in the generating functional in order to obtain equations involving the two-point Green's function in a two-particle irreducible fashion.

The generator of the connected Green's functions is

$$W[\eta,K]=-i\ln Z[\eta,K], \quad (3)$$

and the derivative

$$\frac{\delta W}{\delta\eta_i(\mathbf{r},t)}=\overline{\phi}_i(\mathbf{r},t) \quad (4)$$

gives the average field $\overline{\phi}$ with respect to the action $S[\phi]+\eta^\dagger\phi+\phi^\dagger K\phi/2$,

$$\overline{\phi}(\mathbf{r},t)=\begin{pmatrix}\Phi(\mathbf{r},t)\\ \Phi^*(\mathbf{r},t)\end{pmatrix} =\int\mathcal{D}\phi\,\phi(\mathbf{r},t)\exp\left(iS[\phi]+i\eta^\dagger\phi+\frac{i}{2}\phi^\dagger K\phi\right) =\langle\phi(\mathbf{r},t)\rangle. \quad (5)$$

The average field Φ is seen to specify the condensate density and is referred to as the condensate wave function.

The derivative of W with respect to the two-particle source is

$$\frac{\delta W}{\delta K_{ij}(\mathbf{r},t;\mathbf{r}',t')}=\frac{1}{2}\overline{\phi}_i(\mathbf{r},t)\overline{\phi}_j(\mathbf{r}',t')+\frac{i}{2}G_{ij}(\mathbf{r},t,\mathbf{r}',t'), \quad (6)$$

where G is the full connected two-point matrix Green's function describing the bosons not in the condensate,

$$G_{ij}(\mathbf{r},t,\mathbf{r}',t')=-\frac{\delta^2W}{\delta\eta_i(\mathbf{r},t)\delta\eta_j(\mathbf{r}',t')} =-i\begin{pmatrix}\langle\delta\psi(\mathbf{r},t)\delta\psi^\dagger(\mathbf{r}',t')\rangle & \langle\delta\psi(\mathbf{r},t)\delta\psi(\mathbf{r}',t')\rangle\\ \langle\delta\psi^\dagger(\mathbf{r},t)\delta\psi^\dagger(\mathbf{r}',t')\rangle & \langle\delta\psi^\dagger(\mathbf{r},t)\delta\psi(\mathbf{r}',t')\rangle\end{pmatrix}, \quad (7)$$

where $\delta\psi(\mathbf{r},t)$ is the deviation of the field from its mean value, $\delta\psi=\psi-\Phi$. Likewise, we shall write $\phi=\overline{\phi}+\delta\phi$ for the two-component field. We note that in the path-integral representation, averages over fields, such as in Eq. (7), are automatically time ordered.

We introduce the effective-action Γ, the generator of the two-particle irreducible vertex functions, through the Legendre transform of the generator of connected Green's-functions, W

$$\Gamma[\overline{\phi},G]=W[\eta,K]-\eta^\dagger\overline{\phi}-\frac{1}{2}\overline{\phi}^\dagger K\overline{\phi}-\frac{i}{2}\mathrm{Tr}\,GK. \quad (8)$$

The effective action satisfies the equations $\delta\Gamma/\delta\overline{\phi}=-\eta-K\overline{\phi}$ and $\delta\Gamma/\delta G=-iK/2$. In a physical state where the external sources vanish, $\eta=0=K$, the variations of the effective action with respect to the field averages $\overline{\phi}$ and G vanish, yielding the equations of motion

$$\frac{\delta\Gamma}{\delta\overline{\phi}}=0, \quad (9a)$$

$$\frac{\delta\Gamma}{\delta G}=0. \quad (9b)$$

According to Cornwall *et al.* [16], the effective action can be written on the form

$$\Gamma[\bar{\phi},G]=S[\bar{\phi}]+\frac{i}{2}\mathrm{Tr}\ln G_0G^{-1}+\frac{i}{2}\mathrm{Tr}(G_0^{-1}-\Sigma^{(1)})G - \frac{i}{2}\mathrm{Tr}\,1+\Gamma_2[\bar{\phi},G], \tag{10}$$

where G_0 is the noninteracting matrix Green's function

$$G_0^{-1}(\mathbf{r},t,\mathbf{r}',t')=-\begin{pmatrix} i\partial_t-H_0+\mu & 0 \\ 0 & -i\partial_t-H_0+\mu \end{pmatrix} \times\delta(\mathbf{r}-\mathbf{r}')\,\delta(t-t'), \tag{11}$$

and the matrix

$$\Sigma^{(1)}(\mathbf{r},t,\mathbf{r}',t')=-\frac{\delta^2S}{\delta\phi^\dagger(\mathbf{r},t)\,\delta\phi(\mathbf{r}',t')}\bigg|_{\phi=\bar{\phi}} +G_0^{-1}(\mathbf{r},t,\mathbf{r}',t'), \tag{12}$$

will turn out to be the self energy to one-loop order [see Eq. (21)]. Using the action describing the bosons Eq. (1), we obtain for the components $\Sigma_{ij}^{(1)}(\mathbf{r},t,\mathbf{r}',t')=\delta(t-t')\Sigma_{ij}^{(1)}(\mathbf{r},\mathbf{r}')$, where

$$\Sigma_{11}^{(1)}(\mathbf{r},\mathbf{r}')=\delta(\mathbf{r}'-\mathbf{r})\int d\mathbf{r}''U(\mathbf{r}-\mathbf{r}'')|\Phi(\mathbf{r}'',t)|^2 +U(\mathbf{r}-\mathbf{r}')\Phi^*(\mathbf{r}',t)\Phi(\mathbf{r},t),$$

$$\Sigma_{12}^{(1)}(\mathbf{r},\mathbf{r}')=U(\mathbf{r}-\mathbf{r}')\Phi(\mathbf{r},t)\Phi(\mathbf{r}',t),$$

$$\Sigma_{21}^{(1)}(\mathbf{r},\mathbf{r}')=U(\mathbf{r}-\mathbf{r}')\Phi^*(\mathbf{r},t)\Phi^*(\mathbf{r}',t),$$

$$\Sigma_{22}^{(1)}(\mathbf{r},\mathbf{r}')=\delta(\mathbf{r}'-\mathbf{r})\int d\mathbf{r}''U(\mathbf{r}-\mathbf{r}'')|\Phi(\mathbf{r}'',t)|^2 +U(\mathbf{r}-\mathbf{r}')\Phi^*(\mathbf{r},t)\Phi(\mathbf{r}',t). \tag{13}$$

The delta function in the time coordinates reflects the fact that the interaction is instantaneous. Finally, the quantity Γ_2 in Eq. (10) is

$$\Gamma_2[\bar{\phi},G]=-i\ln\langle e^{iS_{\mathrm{int}}[\bar{\phi},\delta\phi]}\rangle_G^{\mathrm{2PI}}, \tag{14}$$

where $S_{\mathrm{int}}[\bar{\phi},\delta\phi]$ denotes the part of the action $S[\bar{\phi}+\delta\phi]$ which is higher than second order in $\delta\phi$ in an expansion around the average field. The quantity Γ_2 is conveniently described in terms of the diagrams generated by the action $S_{\mathrm{int}}[\bar{\phi},\delta\phi]$, and consists of all the two-particle irreducible vacuum diagrams as indicated by the superscript "2PI," and the diagrams will therefore contain two or more loops. The subscript indicates that propagator lines represent the full Green's-function G, i.e., the brackets with subscript G denote the average

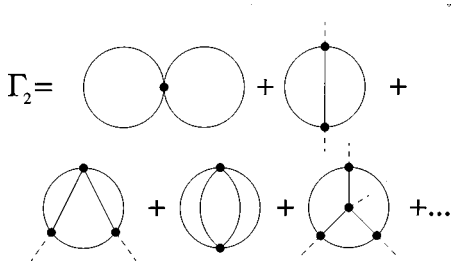

FIG. 1. Two-loop (upper row) and three-loop (lower row) vacuum diagrams contributing to the effective action.

$$\langle e^{iS_{\mathrm{int}}[\bar{\phi},\delta\phi]}\rangle_G=(\det iG)^{-1/2}\int\mathcal{D}(\delta\phi) \times e^{i/2\delta\phi^\dagger G^{-1}\delta\phi}e^{iS_{\mathrm{int}}[\bar{\phi},\delta\phi]}. \tag{15}$$

The diagrammatic expansion of Γ_2 corresponding to the action for the bosons Eq. (1) is illustrated in Fig. 1 where the two- and three-loop vacuum diagrams are shown. Since matrix indices are suppressed, the diagrams are to be understood as follows. Full lines represent the Green's functions and in the cases where we display the different components explicitly, G_{11} will carry one arrow [G_{22} can, according to Eq. (7), be expressed in terms of G_{11} and thus needs no special symbol], G_{12} has two arrows pointing inward, and G_{21} carries two arrows pointing outward. Dashed lines represent the condensate wave function and can also be decorated with arrows, directed out from the vertex to represent Φ, or directed towards the vertex representing Φ^*. The dots where four lines meet are interaction vertices, i.e., they represent the interaction potential U (which in other contexts will be represented by a wiggly line). When all possibilities for the indices are exhausted, subject to the condition that each vertex has two ingoing and two outgoing particle lines, we have represented all the terms of Γ_2 to a given loop order. Finally, the expression corresponding to each vacuum diagram should be multiplied by the factor i^{s-2}, where s is the number of loops the diagram contains. In the effective-action approach, the appearance of the condensate wave function in the diagrams is automatic, and the approach is thus well suited to describe broken-symmetry states.

It is well known that the expansion of the effective action in loop orders is an expansion in Planck's constant $\hbar$ [16]. The first term $S[\bar{\phi}]$ on the right-hand side of Eq. (10) is referred to as the zero-loop term and the terms where the trace is written explicitly as one-loop terms, and they are proportional to $\hbar^0$ and $\hbar^1$, respectively. We note that the presented effective-action approach is capable of describing arbitrary states, including nonequilibrium situations where the external potential depends on time. Although we in the present paper shall limit ourselves to study a Bose gas at zero temperature, the theory is straightforwardly generalized to finite temperatures. For example, in the Schwinger-Keldysh technique for treating general nonequilibrium states, the field is just attributed an additional index. For an account of treating arbitrary states, we refer to Ref. [17]; see also Ref. [18] for an application of the Schwinger-Keldysh technique to the

dilute Bose gas. The equations of motion (9a)–(9b) together with the expression for the effective action Eq. (10) form the basis for our subsequent calculations.

III. HOMOGENEOUS BOSE GAS

We shall now consider the case of a homogeneous Bose gas in equilibrium. The equilibrium theory of a dilute Bose gas is well known, but the effective action formalism will prove to be a simple and efficient tool which permits one to derive the equations of motion with particular ease, and to establish the limits of validity for the approximate descriptions often used. For the case of a homogeneous Bose gas in equilibrium, the general theory presented in the previous section simplifies considerably. The single-particle Hamiltonian H_0 is then simply equal to the kinetic term, $H_0(\mathbf{p})=\mathbf{p}^2/2m \equiv \varepsilon_{\mathbf{p}}$, and the condensate wave-function $\Phi(\mathbf{r},t)$ is a time and coordinate-independent constant whose value is denoted by $\sqrt{n_0}$, so that n_0 denotes the condensate density. The first term in the effective-action Eq. (10) is then

$$S[\Phi]=\left(\mu n_0-\frac{1}{2}U_0 n_0^2\right)\int d\mathbf{r}dt1, \tag{16}$$

where $U_0=\int d\mathbf{r}U(\mathbf{r})$ is the zero-momentum component of the interaction potential. For a constant value of the condensate wave function $\Phi(\mathbf{r},t)=\sqrt{n_0}$, Eq. (13) yields

$$\Sigma^{(1)}(\mathbf{p})=\begin{pmatrix} n_0(U_0+U_{\mathbf{p}}) & n_0U_{\mathbf{p}} \\ n_0U_{\mathbf{p}} & n_0(U_0+U_{\mathbf{p}}) \end{pmatrix}. \tag{17}$$

Varying, in accordance with Eq. (9a), the effective-action Eq. (10) with respect to n_0 yields the equation for the chemical potential

$$\mu=n_0U_0+\frac{i}{2}\int\frac{d^4p}{(2\pi)^4}\{(U_0+U_{\mathbf{p}})[G_{11}(p)+G_{22}(p)] + U_{\mathbf{p}}[G_{12}(p)+G_{21}(p)]\}-\frac{\delta\Gamma_2}{\delta n_0}, \tag{18}$$

where the notation for the four-momentum $p=(\mathbf{p},\omega)$ has been introduced. The first term on the right-hand side is the zero-loop result, which depends only on the condensate fraction of the bosons. The second term on the right-hand side is the one-loop term which takes the noncondensate fraction of the bosons into account. The term involving the anomalous Green's functions G_{12} and G_{21} will shortly be absorbed by the renormalization of the interaction potential (see Sec. IV). From the last term originate the higher-order loop terms which will be dealt with at the end of the section.

The equation determining the Green's function is obtained by varying the effective action with respect to the matrix Green's-function $G(p)$ in accordance with Eq. (9b), yielding

$$0=\frac{\delta\Gamma}{\delta G}=-\frac{i}{2}(-G^{-1}+G_0^{-1}+\Sigma^{(1)}+\Sigma'), \tag{19}$$

where

$$\Sigma'_{ij}=2i\frac{\delta\Gamma_2}{\delta G_{ji}}. \tag{20}$$

Introducing the notation for the matrix self-energy $\Sigma=\Sigma^{(1)}+\Sigma'$, Eq. (19) is seen to be the Dyson equation

$$G^{-1}=G_0^{-1}-\Sigma. \tag{21}$$

In the context of the dilute Bose gas, this equation is referred to as the Dyson-Beliaev equation.

The Green's function in momentum space is obtained by simply inverting the 2×2 matrix $G_0^{-1}(p)-\Sigma(p)$ resulting in the following components:

$$G_{11}(p)=\frac{\omega+\varepsilon_{\mathbf{p}}-\mu+\Sigma_{22}(p)}{D_p},$$

$$G_{12}(p)=\frac{-\Sigma_{12}(p)}{D_p},$$

$$G_{21}(p)=\frac{-\Sigma_{21}(p)}{D_p},$$

$$G_{22}(p)=\frac{-\omega+\varepsilon_{\mathbf{p}}-\mu+\Sigma_{11}(p)}{D_p}, \tag{22}$$

all having the common denominator

$$D_p=[\omega+\varepsilon_{\mathbf{p}}-\mu+\Sigma_{22}(p)][\omega-\varepsilon_{\mathbf{p}}+\mu-\Sigma_{11}(p)] +\Sigma_{12}(p)\Sigma_{21}(p). \tag{23}$$

From the expression for the matrix Green's-function Eq. (7), it follows that in the homogeneous case its components obey the relationships $G_{22}(p)=G_{11}(-p)$ and $G_{12}(-p)=G_{12}(p)=G_{21}(p)$. The corresponding relations hold for the self-energy components. We note that the results found for μ and G to zero- and one-loop order coincide with those found in Ref. [4] to zeroth and first order in the diluteness parameter $\sqrt{n_0a^3}$. For example, according to Eq. (17) we obtain for the components of the matrix Green's function to one-loop order

$$G_{11}^{(1)}(p)=\frac{\omega+\varepsilon_{\mathbf{p}}+n_0U_{\mathbf{p}}}{\omega^2-\varepsilon_{\mathbf{p}}^2-2n_0U_{\mathbf{p}}\varepsilon_{\mathbf{p}}},$$

$$G_{12}^{(1)}(p)=\frac{-n_0U_{\mathbf{p}}}{\omega^2-\varepsilon_{\mathbf{p}}^2-2n_0U_{\mathbf{p}}\varepsilon_{\mathbf{p}}}, \tag{24}$$

which are the same expressions as the ones in Ref. [4]. As we shortly demonstrate, the loop expansion for the case of a homogeneous Bose gas is in fact equivalent to an expansion in the diluteness parameter. From Eq. (24) we obtain for the single-particle excitation energies to one-loop order $E_{\mathbf{p}}=\sqrt{\varepsilon_{\mathbf{p}}^2+2n_0U_{\mathbf{p}}\varepsilon_{\mathbf{p}}}$, which are the well-known Bogoliubov energies [1].

Differentiating with respect to n_0 the terms in Γ_2 corresponding to the two-loop vacuum diagrams gives the two-loop contribution to the chemical potential. Functionally dif-

ferentiating the same terms with respect to G_{ji} gives the two-loop contributions to the self-energies Σ_{ij}. The diagrams we thus obtain for the chemical potential μ and the self-energy Σ are topologically identical to those found by Beliaev [5]; however, the interpretation differs in that the propagator in the vacuum diagrams of Fig. 1 is the exact propagator, whereas in Ref. [5], the propagator to one-loop order appears.

In order to establish that the loop expansion for a homogeneous Bose gas is an expansion in the diluteness parameter $\sqrt{n_0 a^3}$, we examine the general structure of the vacuum diagrams comprised by Γ_2. Any diagram of a given loop order differs from any diagram in the preceding loop order by an extra four-momentum integration, the condensate density n_0 to some power k, the interaction potential U to the power $k+1$, and $k+2$ additional Green's functions in the integrand. We can estimate the contribution from these terms as follows. The Green's functions are approximated by the one-loop result Eq. (24). The additional frequency integration over a product of $k+2$ Green's functions yields $k+2$ factors of $n_0 U$ (where U denotes the typical magnitude of the Fourier transform of the interaction potential), divided by $2k+3$ factors of the Bogoliubov energy E. The range of the momentum integration provided by the Green's functions is $(mn_0U)^{1/2}$. The remaining three-momentum integration therefore gives a factor of order $n_0^{-k+1/2}m^{3/2}U^{-k+1/2}$, and provided the Green's functions make the integral converge, the contribution from an additional loop is of the order $(n_0 m^3 U^3)^{1/2}$. This is the case except for the so-called ladder diagrams, in which case the convergence needs to be provided by the momentum dependence of the potential. The ladder diagrams will be dealt with separately in the next section where we show that they, through a renormalization of the interaction potential, lead to the appearance of the t matrix which in the dilute limit is proportional to the s-wave scattering length a and inversely proportional to the boson mass. The renormalization of the interaction potential will therefore not change the estimates performed above, but only change the expansion parameter. Anticipating this change we conclude that the expansion parameter governing the loop expansion is for a homogeneous Bose gas indeed identical to Bogoliubov's diluteness parameter $\sqrt{n_0 a^3}$.

IV. RENORMALIZATION OF THE INTERACTION

Instead of having the interaction potential appear explicitly in diagrams, one should work in the skeleton diagrammatic representation where diagrams are summed so that the four-point vertex appears instead of the interaction potential, thus accounting for the repeated scattering of the bosons. In the dilute limit, where the interparticle distance is large compared to the s-wave scattering length, the so-called ladder diagrams give the largest contribution to the four-point vertex function [19]. The ladder diagrams are depicted in Fig. 2. On computing the corresponding integrals, it is found that an extra "rung" in a ladder contributes with a factor proportional not to $\sqrt{n_0 m^3 U^3}$ as was the case for the type of extra loops considered at the end of the previous section, but to $k_0 mU$, where k_0 is the upper cutoff momentum (or inverse

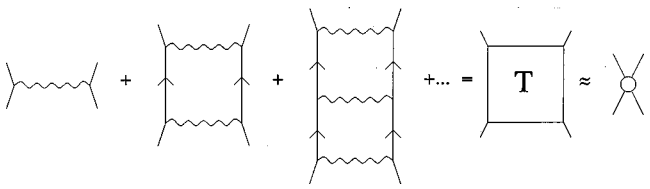

FIG. 2. Summing all diagrams of the "ladder"-type results in the t matrix, which to lowest order in the diluteness parameter is a momentum-independent constant g, diagrammatically represented by a circle.

spatial range) of the potential, as first noted by Beliaev [5]. The quantity $k_0 mU$ is not necessarily small for the atomic gases under consideration here. Hence, all vacuum diagrams which differ only in the number of ladder rungs that they contain are of the same order in the diluteness parameter, and we have to perform a summation over this infinite class of diagrams. The ladder resummation results in an effective potential $T(p,p',q)$, which is called the t matrix and is a function of the two ingoing momenta and the four-momentum transfer. Due to the instantaneous nature of the interactions, the t matrix does not depend on the frequency components of the ingoing four-momenta, but for notational convenience, we display the dependence as $T(p,p',q)$. To lowest order in the diluteness parameter, the t matrix is independent of four-momenta and proportional to the constant scattering amplitude $T(0,0,0)=4\pi\hbar^2 a/m=g$, where a is the s-wave scattering length [19,20]. This is illustrated in Fig. 2, where we have chosen an open circle to represent g. Iterating the equation for the ladder diagrams we obtain the well-known t-matrix equation

$$T(p,p',q)=U_{\mathbf{q}}+i\int d^4q' U_{\mathbf{q}'}G_{11}(p+q')G_{11}(p'-q') \times T(p+q',p'-q',q-q'). \tag{25}$$

At finite temperatures, the t matrix takes into account the effects of thermal population of the excited states.

We shall now show how the ladder resummation alters the diagrammatic representation of the chemical potential and the self energy. In Fig. 3, displayed are some of the terms up to two-loop order contributing to the chemical potential μ.

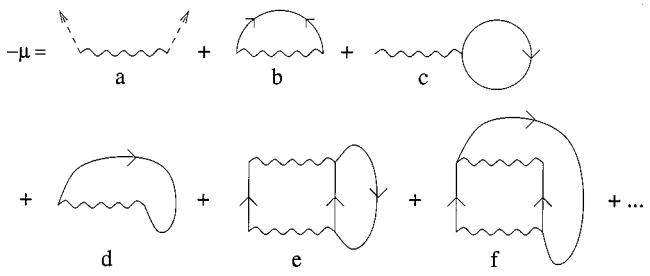

FIG. 3. Diagrams up to two-loop order contributing to the chemical potential. Only the two-loop diagrams relevant to the resummation of the ladder diagrams are displayed. The two-loop diagrams not displayed are topologically identical to those shown, but differ in the direction of arrows or the presence of anomalous instead of normal propagators.

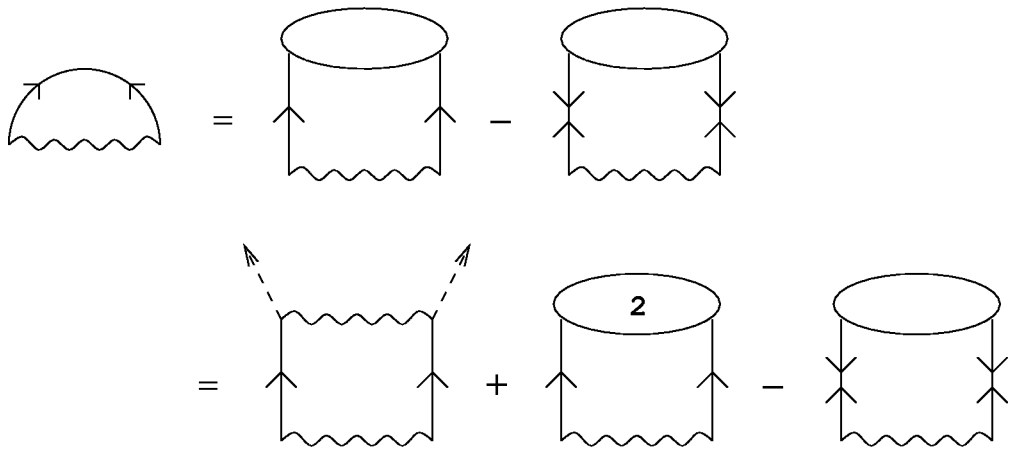

FIG. 4. Diagrammatic representation of the last two rewritings in Eq. (26) which lead to the conclusion that the diagram *b* of Fig. 3 implicitly contains the ladder contribution to diagram *a*. The anomalous self-energy Σ_{12} is represented by an oval with two ingoing lines, Σ_{21} is represented by an oval with two outgoing lines, and the sum of the second- and higher-order contributions to Σ_{12} is represented by an oval with the label "2."

The first two terms in Eq. (18) is represented by diagrams *a*–*d*, and the two-loop diagrams *e*–*f* originate from Γ_2. The diagrams denoted *e* and *f* are formally one loop order higher than *c* and *d*, but they differ only by containing one additional ladder rung. Hence, the diagrams *c*, *d*, *e*, and *f*, and all the diagrams that can be constructed from these by adding ladder rungs, are of the same order in the diluteness parameter $\sqrt{n_0 a^3}$ as just shown above. They are therefore resummed, and as discussed, this leads to the replacement of the interaction potential *U* by the *t* matrix.

We note that no ladder counterparts to the diagrams *a* and *b* in Fig. 3 appear explicitly in the expansion of the chemical potential, since such diagrams are two-particle reducible and are by construction excluded from the two-particle irreducible effective action Γ_2. However, diagram *b* contains implicitly the ladder contribution to diagram *a*. In order to establish this we first simplify the notation by denoting by N_p the numerator of the exact normal Green's function $G_{11}(p)$, which according to Eq. (22) is $N_p = \omega + \varepsilon_{\mathbf{p}} - \mu + \Sigma_{11}(-p)$. We then have $D_p = N_p N_{-p} - \Sigma_{12}(p)\Sigma_{21}(p) = D_{-p}$, and the contribution from diagram b can be rewritten on the forms

$$
\begin{aligned}
&\int d^4p\, U_{\mathbf{p}} G_{12}(p) \\
&\quad = \int d^4p\, U_{\mathbf{p}} \frac{\Sigma_{12}(p)}{N_p N_{-p} - \Sigma_{12}(p)\Sigma_{21}(p)} \\
&\quad = \int d^4p\, U_{\mathbf{p}} \left(\frac{\Sigma_{12}(p) N_p N_{-p}}{D_p^2} - \frac{\Sigma_{12}(p)\Sigma_{21}(p)\Sigma_{12}(p)}{D_p^2} \right) \\
&\quad = \int d^4p\, U_{\mathbf{p}} [\Sigma_{12}(p) G_{11}(p) G_{11}(-p) - \Sigma_{21}(p) G_{12}(p)^2] \\
&\quad = \int d^4p\, U_{\mathbf{p}} \{ n_0 U_{\mathbf{p}} G_{11}(p) G_{11}(-p) + [\Sigma_{12}(p) - n_0 U_{\mathbf{p}}] \\
&\qquad \times G_{11}(p) G_{11}(-p) - \Sigma_{21}(p) G_{12}(p)^2 \}. \qquad (26)
\end{aligned}
$$

In Fig. 4, the last two rewritings are depicted diagrammatically. We see immediately that the first term on the right-hand side corresponds to the first ladder contribution to diagram a, and since to one-loop order, $\Sigma_{12}(p) = n_0 U_{\mathbf{p}}$, the other terms in Eq. (26) are of two- and higher-loop order. The self energy in the second term on the right-hand side can be expanded to second-loop order, and by iteration this yields all the ladder terms, and the remainder can be kept track of analogously to the way in which it is done in Eq. (26). The resulting ladder resummed diagrammatic expression for the chemical potential, displayed in Fig. 5, is seen to be equal to that found in Ref. [19].

In the same manner, the self energies are resummed. For Σ_{11}, a straightforward ladder resummation of all terms is possible, while for Σ_{12}, the same procedure as the one used for diagrams a and b in Fig. 3 for the chemical potential has to be performed. In Fig. 6, we show the resulting ladder resummed diagrams for the self-energies Σ_{11} and Σ_{12} to two-loop order in the dilute limit where $T(p,p',q) \approx g$.

In Ref. [7], a diagrammatic expansion in the potential was performed, which yields to first order the diagram $\Sigma_{11}^{(2a)}$ in Fig. 6, but not the other two-loop diagrams. This theory, where the normal self-energy is taken to be $\Sigma_{11} = \Sigma_{11}^{(1a)} + \Sigma_{11}^{(2a)}$, the anomalous self energy to $\Sigma_{12} = \Sigma_{12}^{(1a)}$, and the diagrams displayed in Fig. 5 are kept in the expansion of the chemical potential, is referred to as the Popov approximation. Although we showed at the end of Sec. III that all the two-loop diagrams of Fig. 6 are of the same order of magnitude in the diluteness parameter $\sqrt{n_0 a^3}$ at zero temperature,

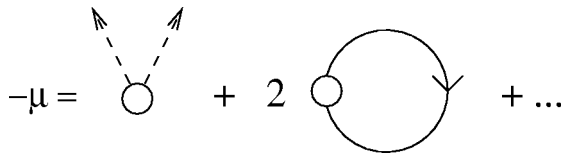

FIG. 5. The chemical potential to one-loop order after the ladder summation has been performed and the resulting *t* matrix has been replaced by its expression in the dilute limit, the constant *g*.

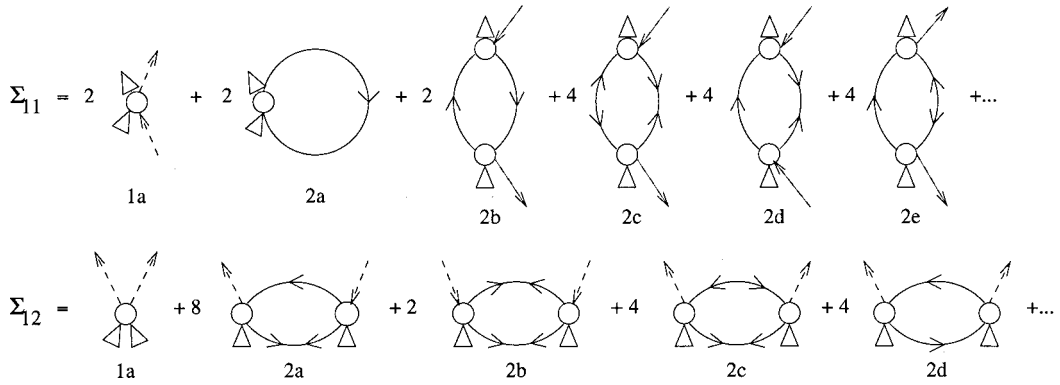

FIG. 6. Normal Σ_{11} and anomalous, Σ_{12} self-energies to two-loop order after the ladder summation has been performed and the resulting t matrix been replaced by its expression in the dilute limit, the constant g.

the Popov approximation applied at finite temperatures is justified, when the temperature is high enough, $kT \gg gn_0$. Below, we shall investigate the limits of validity at zero temperature of the Popov approximation in the trapped case.

In this and the preceding section, we have shown how the known expressions for the self energies and chemical potential for a homogeneous dilute Bose gas are conveniently obtained using the effective action formalism, where they simply correspond to working to a particular order in the loop expansion of the effective action. We have established that an expansion in the diluteness parameter is equivalent to an expansion of the effective action in the number of loops. Furthermore, the method provided a way of performing a systematic expansion, and the results are easily generalized to finite temperatures. We now turn to show that the effective action approach provides a way of performing a systematic expansion even in the case of an inhomogeneous Bose gas.

V. INHOMOGENEOUS BOSE GAS

We now consider the experimentally relevant case of a Bose gas trapped in an external static potential, thereby setting the stage for the numerical calculations in Sec. VI. In this case, the Bose gas will be spatially inhomogeneous. The effective action formalism is equally capable of dealing with the inhomogeneous gas, in which case all quantities are conveniently expressed in configuration space as presented in Sec. II. We show in this section that the Bogoliubov and Gross-Pitaevskii theory corresponds to the one-loop approximation to the effective action. The one-loop equations will be exploited further in the numerical calculations in Sec. VI.

Varying, in accordance with Eq. (9a), the effective action Γ, Eq. (10), with respect to $\Phi^*(\mathbf{r},t)$, we obtain the equation of motion for the condensate wave function

$$(i\hbar\partial_t - H_0 + \mu)\Phi(\mathbf{r},t) = g|\Phi(\mathbf{r},t)|^2\Phi(\mathbf{r},t) + 2igG_{11}(\mathbf{r},t,\mathbf{r},t)\Phi(\mathbf{r},t) - \frac{\delta\bar{\Gamma}_2}{\delta\Phi^*(\mathbf{r},t)}. \quad (27)$$

To zero-loop order, where only the first term on the right-hand side appears, the equation is the time-dependent Gross-Pitaevskii equation [2,3]. We have already, as elaborated in the previous section, performed the ladder summation by which the potential is renormalized and the t matrix appears and have substituted for it the lowest-order approximation in the diluteness parameter, the constant g. Since the t matrix in the momentum variables is a constant in the dilute limit, it becomes in configuration space a product of three delta functions, $T(\mathbf{r}_1,\mathbf{r}_2,\mathbf{r}_3,\mathbf{r}_4) = g\,\delta(\mathbf{r}_1-\mathbf{r}_4)\,\delta(\mathbf{r}_2-\mathbf{r}_4)\,\delta(\mathbf{r}_3-\mathbf{r}_4)$. The quantity $\bar{\Gamma}_2$ is defined as the effective action obtained from Γ_2 by summing the ladder terms whereby U is replaced by the t matrix, and its diagrammatic expansion is topologically of two-loop and higher order.

The Dyson-Beliaev equation, Eq. (21), and the equation determining the condensate wave function, Eq. (27), form a set of coupled integrodifferential self-consistency equations for the condensate wave function and the Green's function, with the self energy specified in terms of the Green's function through Eq. (20). The Green's function can be conveniently expanded in the amplitudes of the elementary excitations. We write the Dyson-Beliaev equation, Eq. (21), on the form

$$\int d\mathbf{r}''dt''[i\hbar\partial_t\sigma_3\delta(\mathbf{r}-\mathbf{r}'')\delta(t-t'') + \sigma_3 L(\mathbf{r},t,\mathbf{r}'',t'')] \times G(\mathbf{r}'',t'',\mathbf{r}',t') = \hbar 1\,\delta(\mathbf{r}-\mathbf{r}')\,\delta(t-t'), \quad (28)$$

where we have introduced the matrix operator $L(\mathbf{r},t,\mathbf{r}',t') = \sigma_3 H_0\delta(\mathbf{r}-\mathbf{r}')\delta(t-t') + \sigma_3\Sigma(\mathbf{r},t,\mathbf{r}',t')$ and σ_3 is a Pauli matrix. Up to one-loop order, the matrix Σ is diagonal in the time and space coordinates and we factor out the delta functions and write $L(\mathbf{r},t,\mathbf{r}',t') = \delta(t-t')\,\delta(\mathbf{r}-\mathbf{r}')L(\mathbf{r})$, where

$$L(\mathbf{r}) = \begin{pmatrix} H_0 - \mu + 2g|\Phi(\mathbf{r})|^2 & g\Phi(\mathbf{r})^2 \\ -g\Phi^*(\mathbf{r})^2 & -H_0 + \mu - 2g|\Phi(\mathbf{r})|^2 \end{pmatrix}. \quad (29)$$

The eigenvalue equation for L are the Bogoliubov equations [1]. The Bogoliubov operator L is not Hermitian, but the operator $\sigma_3 L$ is, which renders the eigenvectors of L the

following properties [22–24]. For each eigenvector $\varphi_j(\mathbf{r}) = (u_j(\mathbf{r}), v_j(\mathbf{r}))$ of L with eigenvalue E_j, there exists an eigenvector $\tilde{\varphi}_j(\mathbf{r}) = (v_j^*(\mathbf{r}), u_j^*(\mathbf{r}))$ with eigenvalue $-E_j$. Assuming the Bose gas is in its ground state, the normalization of the positive-eigenvalue eigenvectors can be chosen to be $\langle \varphi_j, \varphi_k \rangle = \delta_{jk}$ where we have introduced the inner product

$$\langle \varphi_j, \varphi_k \rangle = \int d\mathbf{r} \varphi_j^\dagger(\mathbf{r}) \sigma_3 \varphi_k(\mathbf{r}) = \int d\mathbf{r} [u_j^*(\mathbf{r}) u_k(\mathbf{r}) - v_j^*(\mathbf{r}) v_k(\mathbf{r})]. \quad (30)$$

It follows that the inner product of the negative-eigenvalue eigenvectors $\tilde{\varphi}$ is

$$\langle \tilde{\varphi}_j, \tilde{\varphi}_k \rangle = \int d\mathbf{r} \tilde{\varphi}_j^\dagger(\mathbf{r}) \sigma_3 \tilde{\varphi}_k(\mathbf{r}) = \int d\mathbf{r} [v_j(\mathbf{r}) v_k^*(\mathbf{r}) - u_j(\mathbf{r}) u_k^*(\mathbf{r})] = -\delta_{jk} \quad (31)$$

and the eigenvectors φ and $\tilde{\varphi}$ are mutually orthogonal, $\langle \varphi_j, \tilde{\varphi}_k \rangle = 0$. By virtue of the Gross-Pitaevskii equation, the vector $\varphi_0(\mathbf{r}) = (\Phi(\mathbf{r}), -\Phi^*(\mathbf{r}))$ is an eigenvector of the Bogoliubov operator L with zero eigenvalue and zero norm. In order to obtain a completeness relation, we must also introduce the vector $\varphi_a(\mathbf{r}) = (\Phi_a(\mathbf{r}), -\Phi_a^*(\mathbf{r}))$ satisfying the relation $L\varphi_a = \alpha\varphi_0$, where α is a constant determined by normalization, $\langle \varphi_0, \varphi_a \rangle = 1$ [23]. The resolution of the identity then becomes

$$\sum_j{}' [\varphi_j(\mathbf{r}) \varphi_j^\dagger(\mathbf{r}') - \tilde{\varphi}_j(\mathbf{r}) \tilde{\varphi}_j^\dagger(\mathbf{r}')] \sigma_3 + [\varphi_a(\mathbf{r}) \varphi_0^\dagger(\mathbf{r}') + \varphi_0(\mathbf{r}) \varphi_a^\dagger(\mathbf{r}')] \sigma_3 = 1\, \delta(\mathbf{r} - \mathbf{r}'), \quad (32)$$

where the prime on the summation sign indicates that the zero-eigenvalue mode φ_0 is excluded from the sum. Using the resolution of the identity, Eq. (32), allows us to invert Eq. (28) to obtain the Bogoliubov spectral representation of the Green's function

$$G(\mathbf{r}, \mathbf{r}', \omega) = \hbar \sum_j{}' \left(\frac{1}{-\hbar\omega + E_j} \varphi_j(\mathbf{r}) \varphi_j^\dagger(\mathbf{r}') - \frac{1}{-\hbar\omega - E_j} \tilde{\varphi}_j(\mathbf{r}) \tilde{\varphi}_j^\dagger(\mathbf{r}') \right). \quad (33)$$

It follows from the spectral representation of the Green's function, that the eigenvalues E_j are the elementary excitation energies of the condensed gas (here, constructed explicitly to one-loop order). Using Eq. (33), we can at zero temperature express the noncondensate density or the depletion of the condensate, $n_{\mathrm{nc}} = n - n_0$, in terms of the Bogoliubov amplitudes

$$n_{\mathrm{nc}}(\mathbf{r}) = i \int \frac{d\omega}{2\pi} G_{11}(\mathbf{r}, \mathbf{r}, \omega) = \sum_j{}' |v_j(\mathbf{r})|^2. \quad (34)$$

The results obtained in this section form the basis for the numerical calculations presented in the next section.

VI. LOOP EXPANSION FOR A TRAPPED BOSE GAS

We now turn to determine the validity criteria for the equations obtained to various orders in the loop expansion for the ground state of a Bose gas trapped in an isotropic harmonic potential $V(r) = \frac{1}{2} m \omega_t^2 r^2$. To this end, we shall numerically compute the self-energy diagrams to different orders in the loop expansion.

Working consistently to one-loop order, we need only employ Eq. (27) to zero-loop order, providing the condensate wave function which upon insertion into Eq. (29) yields the Bogoliubov operator L to one-loop order, from which the Green's function to one-loop order is obtained from Eq. (33). The resulting Green's function is then used to calculate the various self-energy terms numerically. In order to do so, we make the equations dimensionless with the transformations $r = a_{\mathrm{osc}} \tilde{r}$, $\Phi = \sqrt{N_0 / a_{\mathrm{osc}}^3} \tilde{\Phi}$, $u_j = a_{\mathrm{osc}}^{-3/2} \tilde{u}_j$, $E_j = \hbar\omega_t \tilde{E}_j$, and $g = (\hbar\omega_t a_{\mathrm{osc}}^3 / N_0) \tilde{g}$, where $a_{\mathrm{osc}} = \sqrt{\hbar / m\omega_t}$ is the oscillator length of the harmonic trap, and N_0 is the number of bosons in the condensate.

To zero-loop order, the time-independent Gross-Pitaevskii equation on dimensionless form reads

$$-\frac{1}{2} \nabla_{\tilde{r}}^2 \tilde{\Phi} + \frac{1}{2} \tilde{r}^2 \tilde{\Phi} + \tilde{g} |\tilde{\Phi}|^2 \tilde{\Phi} = \tilde{\mu} \tilde{\Phi}. \quad (35)$$

We solve Eq. (35) numerically with the steepest-descent method, which has proven to be sufficient for solving the present equation [25]. The result thus obtained for $\tilde{\Phi}$ is inserted into the one-loop expression for the Bogoliubov operator L, Eq. (29), in order to calculate the Bogoliubov amplitudes $\tilde{u}_j$ and $\tilde{v}_j$ and the eigenenergies $\tilde{E}_j$. Since the condensate wave function for the ground-state $\tilde{\Phi}$ is real and rotationally symmetric, the amplitudes $\tilde{u}_j, \tilde{v}_j$ in the Bogoliubov equations can be labeled by the two angular momentum quantum numbers l and m, and a radial quantum number n, and we write $\tilde{u}_{nlm}(\tilde{r}, \theta, \phi) = \tilde{u}_{nl}(\tilde{r}) Y_{lm}(\theta, \phi)$, $\tilde{v}_{nlm}(\tilde{r}, \theta, \phi) = \tilde{v}_{nl}(\tilde{r}) Y_{lm}(\theta, \phi)$. The resulting Bogoliubov equations are linear and one dimensional

$$\left(-\frac{1}{2} \frac{1}{\tilde{r}} \frac{\partial^2}{\partial \tilde{r}^2} \tilde{r} + \frac{1}{2} \frac{l(l+1)}{\tilde{r}^2} + \frac{1}{2} \tilde{r}^2 - \tilde{\mu} + 2\tilde{g} \tilde{\Phi}^2(\tilde{r}) \right) \times \tilde{u}_{nl}(\tilde{r}) + \tilde{g} \tilde{\Phi}^2(\tilde{r}) \tilde{v}_{nl}(\tilde{r}) = \tilde{E}_{nl} \tilde{u}_{nl}(\tilde{r}),$$

$$\left(-\frac{1}{2} \frac{1}{\tilde{r}} \frac{\partial^2}{\partial \tilde{r}^2} \tilde{r} + \frac{1}{2} \frac{l(l+1)}{\tilde{r}^2} + \frac{1}{2} \tilde{r}^2 - \tilde{\mu} + 2\tilde{g} \tilde{\Phi}^2(\tilde{r}) \right) \times \tilde{v}_{nl}(\tilde{r}) + \tilde{g} \tilde{\Phi}^2(\tilde{r}) \tilde{u}_{nl}(\tilde{r}) = -\tilde{E}_{nl} \tilde{v}_{nl}(\tilde{r}). \quad (36)$$

Note that the only parameter in the problem is the dimensionless coupling parameter $\tilde{g}=4\pi N_0 a/a_{\rm osc}$. Solving the Bogoliubov equations reduces to diagonalizing the band diagonal $2M\times 2M$ matrix L, where M is the size of the numerical grid. The value of M in our computations was varied between 180 and 360, higher values for stronger coupling, and the grid constant has been chosen to $0.05a_{\rm osc}$ giving a maximum system size of $18a_{\rm osc}$. We have used MATLAB to perform the diagonalization.

In the following, we shall estimate the orders of magnitude and the parameter dependence of the different two- and three-loop self-energy diagrams, and to this end we shall use the one-loop results for the amplitudes $\tilde{u}$, $\tilde{v}$, and the eigenenergies $\tilde{E}$ obtained numerically. When working to two- and three-loop order, one must also consider the corresponding corrections to the approximate t-matrix g. These contributions have been studied in Ref. [11], and their inclusion will not lead to any qualitative changes of our results. In fact, even at finite temperature, the dependence of the t matrix on the coupling parameter $\tilde{g}$ is weak as long as the temperature is not close to the critical temperature for Bose-Einstein condensation [19,21].

Let us first compare the one-loop and two-loop contributions to the normal self energy. The only one-loop term is

$$\Sigma_{11}^{(1a)}(\mathbf{r},\mathbf{r}',\omega)=2g|\Phi(\mathbf{r})|^2\delta(\mathbf{r}-\mathbf{r}')=2gn_0(\mathbf{r})\delta(\mathbf{r}-\mathbf{r}'). \tag{37}$$

We first compare $\Sigma_{11}^{(1a)}$ with the two-loop term which is proportional to a delta function, i.e., the diagram $2a$ in Fig. 6. We shall shortly compare this diagram to the other two-loop diagrams. For diagram $2a$, we have

$$\Sigma_{11}^{(2a)}(\mathbf{r},\mathbf{r}',\omega)=2ig\,\delta(\mathbf{r}-\mathbf{r}')\int\frac{d\omega'}{2\pi}G(\mathbf{r},\mathbf{r},\omega')$$
$$=2gn_{\rm nc}(\mathbf{r})\delta(\mathbf{r}-\mathbf{r}'). \tag{38}$$

The ratio of the two-loop to one-loop self-energy contributions at the point $\mathbf{r}$ is thus equal to the fractional depletion of the condensate at that point. In Fig. 7, shown is the numerically computed dimensionless fractional depletion at the origin, $\tilde{n}_{\rm nc}(0)/\tilde{n}_0(0)$, where we have introduced the dimensionless notation

$$\tilde{n}_0(\tilde{\mathbf{r}})=|\tilde{\Phi}(\tilde{\mathbf{r}})|^2,$$

$$\tilde{n}_{\rm nc}(\tilde{\mathbf{r}})=\sum_j{}'\ |\tilde{v}_j(\tilde{\mathbf{r}})|^2. \tag{39}$$

We have chosen to evaluate the densities at the origin, $\mathbf{r}=0$, in order to avoid a prohibitively large summation over the $l\neq 0$ eigenvectors. As apparent from Fig. 7, the log-log curve has a slight bend at weak coupling, but becomes almost straight for coupling strengths $\tilde{g}\gtrsim 100$. A logarithmic fit to the straight portion of the curve gives the relation

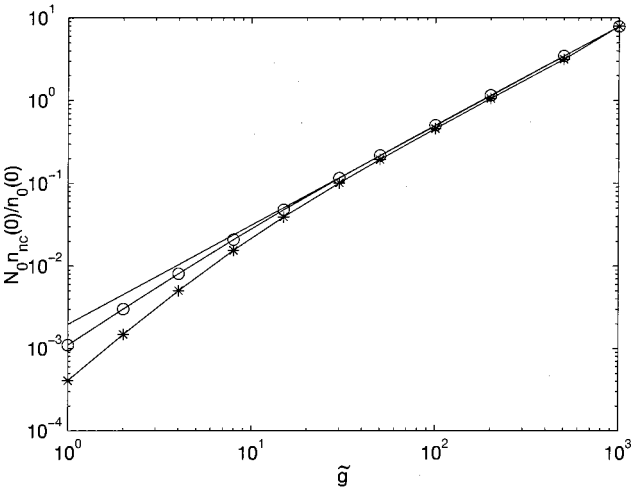

FIG. 7. Fractional depletion of the condensate $N_0 n_{\rm nc}/n_0$ at the trap center as a function of the dimensionless coupling strength $\tilde{g}=4\pi N_0 a/a_{\rm osc}$. Asterisks represent our numerical results, circles represent the local-density approximation with the numerically computed condensate density inserted, and the line is the local-density approximation using the Thomas-Fermi approximation for the condensate density.

$$\frac{\tilde{n}_{\rm nc}(0)}{\tilde{n}_0(0)}\simeq 0.0019\tilde{g}^{1.2}. \tag{40}$$

When we reintroduce dimensions, the power-law relationship Eq. (40) is multiplied by the reciprocal of the number of bosons in the condensate N_0^{-1} because the actual and dimensionless self energies are related according to

$$\Sigma^{(s)}=\frac{\hbar\omega_t a_{\rm osc}^3}{N_0^{s-1}}\tilde{\Sigma}^{(s)}, \tag{41}$$

where s denotes the loop order in question. The ratio between different loop orders of the self energy is thus not determined solely by the dimensionless coupling parameter $\tilde{g}=4\pi N_0 a/a_{\rm osc}$, but by N_0 and $a/a_{\rm osc}$ separately. We thus obtain for the fractional depletion in the strong-coupling limit, $\tilde{g}\gtrsim 100$

$$\frac{n_{\rm nc}(0)}{n_0(0)}=\frac{1}{N_0}\frac{\tilde{n}_{\rm nc}(0)}{\tilde{n}_0(0)}\approx 0.041N_0^{0.2}\left(\frac{a}{a_{\rm osc}}\right)^{1.2}. \tag{42}$$

It is of interest to compare our numerical results with approximate analytical results such as those obtained using the local-density approximation (LDA). The LDA amounts to substituting a coordinate-dependent condensate density in the expressions valid for the homogeneous gas. The homogeneous-gas result for the fractional depletion is [1]

$$\frac{n_{\rm nc}}{n_0}=\frac{8}{3\sqrt{\pi}}\sqrt{n_0 a^3}. \tag{43}$$

In the strong coupling limit we can use the Thomas-Fermi approximation for the condensate density

$$n_0(\mathbf{r}) = \frac{1}{8\pi a_{\rm osc}^2 a}\left(\frac{15N_0 a}{a_{\rm osc}}\right)^{2/5}\left[1-\left(\frac{a_{\rm osc}}{15N_0 a}\right)^{2/5}\frac{r^2}{a_{\rm osc}^2}\right], \tag{44}$$

which is obtained by neglecting the kinetic term in the Gross-Pitaevskii equation [26]. For the fractional depletion at the origin there results in the local-density approximation

$$\frac{n_{\rm nc}(0)}{n_0(0)} = \frac{(15N_0)^{1/5}}{3\pi^2\sqrt{2}}\left(\frac{a}{a_{\rm osc}}\right)^{6/5}, \tag{45}$$

as first obtained in Ref. [27]. The LDA is a valid approximation when the gas locally resembles that of a homogeneous system, i.e., when the condensate wave function changes little on the scale of the coherence length ξ, which according to the Gross-Pitaevskii equation is $\xi=[8\pi n_0(0)a]^{-1/2}$. For a trapped cloud of bosons in the ground state, its radius R determines the rate of change of the density profile. Since R is a factor $\tilde{g}^{2/5}$ larger than ξ [26], we expect the agreement between the LDA and the exact results to be best in the strong-coupling regime. The fractional depletion of the condensate at the trap center as a function of the dimensionless coupling strength $\tilde{g}=4\pi N_0 a/a_{\rm osc}$ is shown in Fig. 7. In Fig. 7 displayed are both the local-density result Eq. (43), with the numerically computed condensate density inserted, and the Thomas-Fermi approximation (45), showing that the LDA indeed is valid when the coupling is strong. Furthermore, inspection of Eq. (45) reveals that the LDA coefficient and exponent agree with the numerically found result of Eq. (42), which is valid for strong coupling. However, when $\tilde{g} \lesssim 10$, the LDA prediction for the depletion deviates significantly from the numerically computed depletion. Using the numerically obtained condensate density in the LDA, instead of the Thomas-Fermi approximation, does not substantially improve the result, as seen in Fig. 7.

The relation for the fractional depletion Eq. (42) is in agreement with the results of Ref. [12], where the leading-order corrections to the Gross-Pitaevskii equation were considered in the one-particle irreducible effective-action formalism, employing physical assumptions about the relevant length scales in the problem. These leading-order corrections were found to have the same power-law dependence on N_0 and $a/a_{\rm osc}$. A direct comparison of the prefactors cannot be made, because the objective of Ref. [12] was to estimate the higher-loop correction terms to the Gross-Pitaevskii equation and not to the self energy.

The two-loop term $\Sigma_{11}^{(2a)}$ can, at zero temperature according to Eq. (40) be ignored as long as $\tilde{n}_{\rm nc} \ll \tilde{n}_0$, which is true in a wide, experimentally relevant parameter regime. The one-loop result for the fractional depletion Eq. (42) depends very weakly on N_0, so as long as N_0 does not exceed 10^9, which is usually fulfilled in experiments, we can restate the criterion for the validity of Eq. (42) into the condition $a \ll a_{\rm osc}$. In experiments on atomic rubidium and sodium condensates, this condition is fulfilled, except in the instances where Feshbach resonances are used to enhance the scattering length [14,15].

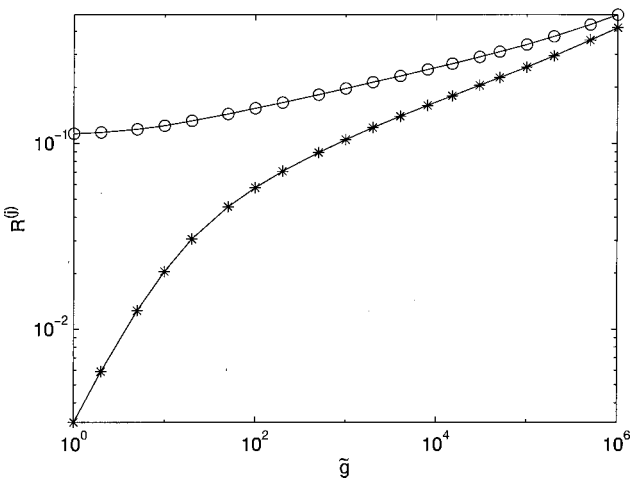

FIG. 8. Ratio between different two-loop self-energy terms as functions of the dimensionless coupling strength $\tilde{g}=4\pi N_0 a/a_{\rm osc}$. Asterisks denote the ratio $R^{(2b)}$ as defined in Eq. (46) and circles denote the ratio $R^{(2c)}$. The terms $R^{(2d)}$ and $R^{(2e)}$ are equal and turn out to be equal in magnitude to $R^{(2b)}$, and are not displayed.

In Sec. III, we showed that for a homogeneous gas all two-loop diagrams are equally important in the sense that they are all of the same order in the diluteness parameter $\sqrt{n_0 a^3}$. The situation in a trapped system is not so clear, since the density is not constant. We shall therefore compare the five normal two-loop self-energy diagrams $\Sigma_{11}^{(2a-2e)}$ in Fig. 6, to see whether they display the same parameter dependences and whether any of the terms can be neglected. In particular, the Popov approximation corresponds to keeping the diagram $\Sigma_{11}^{(2a)}$ but neglects all other two-loop diagrams, and we will now determine its limits of validity at zero temperature. Since diagram $2a$ contains a delta function, we shall integrate over one of the spatial arguments of the self-energy terms and keep the other one fixed at the origin, $\mathbf{r}=0$. We denote by $R^{(j)}$ the ratio between the integrated self-energy terms j and $2a$,

$$R^{(j)} = \frac{\int d\mathbf{r}\Sigma_{11}^{(j)}(0,\mathbf{r},\omega=0)}{\int d\mathbf{r}\Sigma_{11}^{(2a)}(0,\mathbf{r},\omega=0)}. \tag{46}$$

In Fig. 8, we display the ratios $R^{(j)}$ for the different integrated self-energy contributions corresponding to the diagrams where j represents $2b$ and $2c$. The contributions from diagrams $2d$ and $2e$ are equal and within our numerical precision turn out to be equal to the contribution from diagram $2c$. Furthermore, inspection of the diagrams in Fig. 6 reveals that when the condensate wave function is real, the anomalous contribution $\Sigma_{12}^{(2a)}$ is equal to $\Sigma_{11}^{(2d)}$, the diagrams $\Sigma_{12}^{(2b)}$ and $\Sigma_{12}^{(2c)}$ are equal to $\Sigma_{11}^{(2c)}$, and $\Sigma_{12}^{(2d)}$ is equal to $\Sigma_{11}^{(2b)}$. In the parameter regime displayed in Fig. 8, the contribution from diagram 2a is larger than the others by approximately a

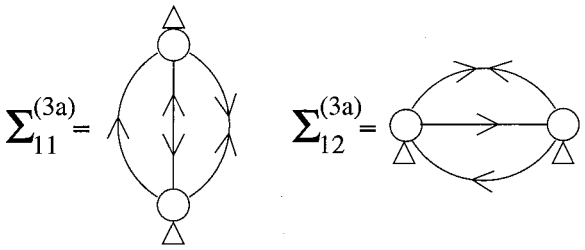

FIG. 9. Self-energy diagrams to three-loop order which are evaluated numerically.

factor of ten, and displays only a weak dependence on the coupling strength. In the weak-coupling limit $\tilde{g} \lesssim 1$, it is seen that the terms corresponding to diagrams $2b-2e$ can be neglected as in the Popov approximation, with an error in the self energy of a few percent. When the coupling gets stronger, this correction becomes more important. A power-law fit to the ratio $R^{(2c)}$ in the regime where the log-log curve is straight yields the dependence

$$R^{(2c)} \approx 0.065 \tilde{g}^{0.14}, \tag{47}$$

which is equal to 0.5 when $\tilde{g} \approx 10^6$; for $\tilde{g}$ greater than this value, the Popov approximation is seen not to be valid. If the ratio between the oscillator length and the scattering length is equal to one hundred, $a_{\mathrm{osc}} = 100a$, the Popov approximation deviates markedly from the two-loop result when N_0 exceeds 10^7, which is often the case experimentally.

In order to investigate the importance of higher-order terms in the loop expansion, we proceed to study the three-loop self-energy diagrams. We have found the number of summations over Bogoliubov levels to be prohibitively large for most three-loop terms; however, we *have* been able to compute the two diagrams $\Sigma_{11}^{(3a)}$ and $\Sigma_{12}^{(3a)}$, displayed in Fig. 9, for the case where one of the spatial arguments is placed at the origin thereby avoiding the summation over $l \neq 0$ components. We compare the diagrams $\Sigma_{11}^{(3a)}$ and $\Sigma_{12}^{(3a)}$ to the two-loop diagrams. As we have seen, diagrams $\Sigma_{11}^{(2b)}$, $\Sigma_{11}^{(2c)}$, and $\Sigma_{11}^{(2d)}$ in Fig. 6 are of the same order of magnitude and have similar dependence on $\tilde{g}$, and equivalently for the anomalous two-loop diagrams $\Sigma_{12}^{(2a-2d)}$; we have therefore chosen to evaluate only diagrams $\Sigma_{11}^{(2b)}$ and $\Sigma_{12}^{(2a)}$. The results for the ratios $\tilde{\Sigma}_{11}^{(3a)}(0,r,\omega=0)/\tilde{\Sigma}_{11}^{(2b)}(0,r,\omega=0)$, and $\tilde{\Sigma}_{12}^{(3a)}(0,r,\omega=0)/\tilde{\Sigma}_{12}^{(2a)}(0,r,\omega=0)$, evaluated for different choices of r, are shown in Fig. 10. A linear fit to the log-log plot gives for the normal terms the coefficient 0.016 and the exponent 0.76 when $r=0.5a_{\mathrm{osc}}$ and the coefficient 0.0029 and the exponent 0.78 when $r=a_{\mathrm{osc}}$, and for the anomalous terms with the choice $r=a_{\mathrm{osc}}$ the coefficient is 0.0015 and the exponent 0.82. Restoring dimensions according to Eq. (41) we obtain

$$\frac{\Sigma_{11}^{(3a)}(0,a_{\mathrm{osc}},\omega=0)}{\Sigma_{11}^{(2b)}(0,a_{\mathrm{osc}},\omega=0)} \approx 0.15 N_0^{-0.2} \left(\frac{a}{a_{\mathrm{osc}}}\right)^{0.8}. \tag{48}$$

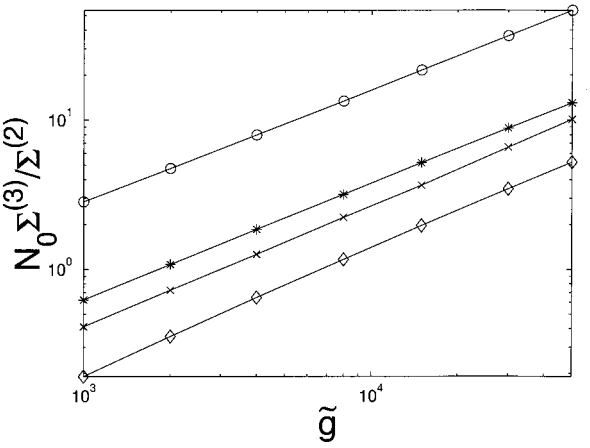

FIG. 10. Ratio of dimensionless three-loop to two-loop self-energy diagrams as a function of the dimensionless coupling strength $\tilde{g}=4\pi N_0 a/a_{\mathrm{osc}}$. Asterisks denote the ratio of the normal self-energy terms $N_0\Sigma_{11}^{(3a)}/\Sigma_{11}^{(2b)}$ evaluated at the point $(0,a_{\mathrm{osc}},\omega=0)$, open circles denote the same ratio evaluated at $(0,0.5a_{\mathrm{osc}},\omega=0)$, and diamonds denote the same ratio evaluated at $(0,1.5a_{\mathrm{osc}},\omega=0)$. Crosses denote the ratio of anomalous self-energy terms $N_0\Sigma_{12}^{(3a)}/\Sigma_{12}^{(2a)}$ at $(0,a_{\mathrm{osc}},\omega=0)$.

The ratio between three- and two-loop self-energy terms in the homogeneous case was in Sec. III found to be proportional to $\sqrt{n_0 a^3}$. A straightforward application of the LDA, substituting the central density $n_0(0)$ for n_0, yields the dependence $\Sigma_{11}^{(3a)}/\Sigma_{11}^{(2b)} \propto N_0^{0.2}(a/a_{\mathrm{osc}})^{1.2}$. This is not in accordance with the numerical result Eq. (48) although the self energies were evaluated at spatial points close to the trap center. The discrepancy between the LDA and the numerical three-loop result is attributed to the fact that we fixed the spatial points in units of a_{osc} while varying the coupling $\tilde{g}$, although the physical situation at the point $r=a_{\mathrm{osc}}$ (and $r=\frac{1}{2}a_{\mathrm{osc}}$ and $r=\frac{3}{2}a_{\mathrm{osc}}$, respectively) varies when $\tilde{g}$ is varied. It is possible that the agreement with the LDA had been better if the length scales had been fixed in units of the actual cloud radius (as given by the Thomas-Fermi approximation) rather than the oscillator length. However, the present calculation agrees fairly well with the LDA as long as the number of atoms in the condensate lies within reasonable bounds. Since $N_0 > 1$ in the condensed state, Eq. (48) yields that $\Sigma_{11}^{(3a)} \ll \Sigma_{11}^{(2b)}$ whenever the s-wave scattering length is much smaller than the trap length. We conclude that only when this condition is not fulfilled is it necessary to study diagrams of three-loop order and beyond.

VII. CONCLUSION

We have applied the two-particle irreducible effective-action approach to a condensed Bose gas, and shown that it allows for an efficient and systematic derivation of the equations of motion both in the homogeneous and trapped case. The presented results are obtained for zero temperature, but the formalism is with equal ease capable of dealing with systems at finite temperatures and general nonequilibrium states. Beliaev's diagrammatic expansion in the diluteness

parameter and the *t*-matrix equations are expediently arrived at with the aid of the effective-action formalism. We have shown that the parameter characterizing the loop expansion for a homogeneous Bose gas is equal to the diluteness parameter, the ratio of the *s*-wave scattering length to the interparticle spacing. For a Bose gas contained in an isotropic, three-dimensional harmonic-oscillator trap at zero temperature, the small parameter governing the loop expansion has been found to be almost proportional to the ratio between the *s*-wave scattering length and the oscillator length of the trapping potential, and to have a weak dependence on the number of particles in the condensate. The expansion to one-loop order, and hence the Bogoliubov equation, is found to provide a valid description for the trapped gas when the oscillator length exceeds the *s*-wave scattering length. We have compared our numerical results with the local-density approximation, which is found to be valid when the number of particles in the condensate is large compared to the ratio between the oscillator length and the *s*-wave scattering length. The physical consequences of the self-energy corrections considered in this paper are indeed possible to study experimentally by using Feshbach resonances to vary the scattering length. Furthermore, we have found that all the self-energy terms of two-loop order are not equally large for the case of a trapped system: in the limit when the number of particles in the condensate is not large compared to the ratio between the oscillator length and the *s*-wave scattering length, the Popov approximation has been shown to be a valid approximation.

ACKNOWLEDGMENTS

It is a pleasure to acknowledge helpful discussions with Lars Melwyn Jensen, Chris Pethick, Henrik Smith, and Stig Stenholm.

[1] N. N. Bogoliubov, J. Phys. (Moscow) **11**, 23 (1947).
[2] E. P. Gross, Nuovo Cimento **20**, 454 (1961); J. Math. Phys. **4**, 195 (1963).
[3] L. P. Pitaevskii, Zh. Éksp. Teor. Fiz. **40**, 646 (1961) [Sov. Phys. JETP **13**, 451 (1961)].
[4] S. T. Beliaev, Zh. Éksp. Teor. Fiz. **34**, 417 (1958) [Sov. Phys. JETP **7**, 289 (1958)].
[5] S. T. Beliaev, Zh. Éksp. Teor. Fiz. **34**, 433 (1958) [Sov. Phys. JETP **7**, 299 (1958)].
[6] V. N. Popov and L. D. Faddeev, Zh. Éksp. Teor. Fiz. **47**, 1315 (1964) [Sov. Phys. JETP **20**, 890 (1965)].
[7] V. N. Popov, Zh. Éksp. Teor. Fiz. **47**, 1759 (1964) [Sov. Phys. JETP **20**, 1185 (1965)].
[8] V. N. Popov, *Functional Integrals and Collective Excitations* (Cambridge University Press, New York, 1987).
[9] M. H. Anderson, J. R. Ensher, M. R. Matthews, C. E. Wieman, and E. A. Cornell, Science **269**, 198 (1995).
[10] N. P. Proukakis, K. Burnett, and H. T. C. Stoof, Phys. Rev. A **57**, 1230 (1998).
[11] N. P. Proukakis, S. A. Morgan, S. Choi, and K. Burnett, Phys. Rev. A **58**, 2435 (1998).
[12] S. Stenholm, Phys. Rev. A **57**, 2942 (1998).
[13] P. O. Fedichev and G. V. Shlyapnikov, Phys. Rev. A **58**, 3146 (1998).
[14] S. Inouye, M. R. Andrews, J. Stenger, H.-J. Miesner, D. M. Stamper-Kurn, and W. Ketterle, Nature (London) **392**, 151 (1998).
[15] S. L. Cornish, N. R. Claussen, J. L. Roberts, E. A. Cornell, and C. E. Wieman, Phys. Rev. Lett. **85**, 1795 (2000).
[16] J. M. Cornwall, R. Jackiw, and E. Tomboulis, Phys. Rev. D **10**, 2428 (1974).
[17] S. Grundberg and J. Rammer, Phys. Rev. B **61**, 699 (2000).
[18] H. T. C. Stoof, J. Low Temp. Phys. **114**, 1 (1999).
[19] H. Shi and A. Griffin, Phys. Rep. **304**, 1 (1988).
[20] H. T. C. Stoof, M. Bijlsma, and M. Houbiers, J. Res. Natl. Inst. Stand. Technol. **101**, 443 (1996).
[21] M. Bijlsma and H. T. C. Stoof, Phys. Rev. A **55**, 498 (1997).
[22] A. L. Fetter, Ann. Phys. (N.Y.) **70**, 67 (1972).
[23] J.-P. Blaizot and G. Ripka, *Quantum Theory of Finite Systems* (MIT Press, Cambridge, MA, 1986).
[24] Y. Castin and R. Dum, Phys. Rev. A **57**, 3008 (1998).
[25] F. Dalfovo and S. Stringari, Phys. Rev. A **53**, 2477 (1996).
[26] G. Baym and C. J. Pethick, Phys. Rev. Lett. **76**, 6 (1996).
[27] F. Dalfovo, S. Giorgini, L. P. Pitaevskii, and S. Stringari, Rev. Mod. Phys. **71**, 463 (1999).